Deep Learning Approach for Heavy Rainfall Prediction Using Himawari-8 And RDCA Data

Muhammad Fadhlan Putranto
School of Electrical Engineering and Informatics, Bandung Institute of Technology
Bandung, Indonesia
23521054@stei.std.itb.ac.id

Rinaldi Munir
School of Electrical Engineering and Informatics, Bandung Institute of Technology
Bandung, Indonesia
rinaldi@informatika.org

Abstract—**High-intensity rainfall in a short period can increase the likelihood of landslides and floods. The disaster mitigation process will be too late in such a short period. The absence of an early warning system also worsens this. Therefore, an accurate prediction system is needed to predict heavy rainfall. By utilizing real-time observation data from Himawari-8, Rapidly Developing Cumulus Area (RDCA) can predict the possibility of heavy rainfall. However, RDCA has not been able to make predictions for a long period. Therefore, we propose a heavy rainfall prediction model from a deep learning perspective in this research by utilizing cloud observation data from Himawari-8 and RDCA index data.**

In this study, a Convolutional Long-Short Term Memory Model (ConvLSTM) with an encoder-forecaster architecture is designed to perform heavy rainfall prediction. The results of the model training process show that the performance increases as the training iterations grow. In addition, in experiments with test data, the model also produces probability values that are close to the same as the RDCA index value. This can be seen from the SSIM value, which is close to one.

Keywords— Rainfall Prediction, Convolutional Long-Short Term Memory, RDCA

I. INTRODUCTION

Natural disasters in Indonesia are dominated by hydrometeorological disasters such as landslides and floods. According to the National Agency for Disaster Countermeasures (BNPB), In 2022, more than 91% of natural disaster events consist of landslides, extern weather, and floods [1]. Both events caused 239 fatalities, 199 injured, and more than 5 million affected. According to Indradewa, the increase in rainfall is related to several meteorological phenomena that have caused hydrometeorological disasters in Indonesia [2]. The meteorological phenomenon in the form of a powerful surface wind flow across the equator, also known as the Cross-Equatorial Northerly Surge (CENS), is closely related to increased rainfall in parts of Indonesia [3]–[5]. Therefore, a prediction system capable of predicting rain is needed. However, making an accurate prediction system, especially for heavy rainfall that occurs in short-term and high intensity, is a considerable challenge.

Many organizations and researchers have made rainfall predictions. Most popular methods use numerical model simulation by predicting the physical processes of the atmosphere by determining the conservation principles of atmospheric mass, energy, and momentum [6]. One of these methods is numerical weather predictions (NWP) [7]. NWP predicts using mathematical models of the atmosphere and ocean based on current weather conditions obtained from radiosondes, satellites, or other weather observation tools. Results: This model can simulate heavy rain events for the long term into the next several days (with a 1-hour step frequency). However, a model that can make short-term predictions is needed to capture flash flood events due to the high intensity of rain in a short period. Several numerical methods developed by previous researchers can solve this short-term prediction problem. This was done by Harjupa et al. using a technique called the Rapidly Development Cumulus Area (RDCA) [8]. This method utilizes Himawari-8 satellite data to obtain the RDCA index value, which states the probability of extreme rai. As a result, the RDCA index can show intense rain 50 minutes before the observed rain in Japan. This method has also been verified in Japan by comparing the RDCA index with cumulus cloud cycles [9] and cloud particle types [10]. This RDCA method has recently been verified in Indonesia, especially in West Java Province. Verification is done by comparing the RDCA index with radar data provided by the Meteorology, Climatology, and Geophysics Agency (BMKG) and the ATMOS41 weather station managed by the Bandung Institute of Technology (ITB). The result is that the RDCA method can detect and predict rain events in the observation area. However, there are still several limitations to heavy rainfall predictions using RDCA-based. RDCA only predicts one result with a 10-minute step frequency. Therefore, a new approach is needed in predicting heavy rainfall, which can result in multiple-step frequency ahead. One of the approaches currently being developed is deep learning.

Deep learning (DL) is designed based on the neural network architecture, which consists of neurons with deep or recursive architectures [11]. The increasing complexity of NNs currently makes DL able to solve problems such as image recognition [12], voice recognition [13], video analysis and prediction [14], [15] from various fields such as medical, transportation, banking, and others [16]–[18]. This is a concern for the meteorological research community in applying DL technology in weather and climatology research, such as predicting the impact of rainfall [19] and forecasting precipitation [20].

In this study, we aim for heavy rainfall prediction using satellite observation (Himawari-8) and RDCA data. Because this data is spatiotemporal, using the DL approach to unravel this problem. Three common DL techniques can be used, i.e., convolutional neural network (CNN) based architectures, recurrent neural network (RNN) based architectures, and their combined architecture and combination of their architecture. This study used a combination of CNN and RNN architecture, namely Convolutional Long-Short Term Memory (ConvLSTM) [21]. This architecture is a combination of CNN [11] and LSTM [22], in which CNN aims to capture spatial features of the image (data) on a global and local scale. In contrast, long-short-term memory (LSTM) aims to extract temporal features of images (data). Therefore, the
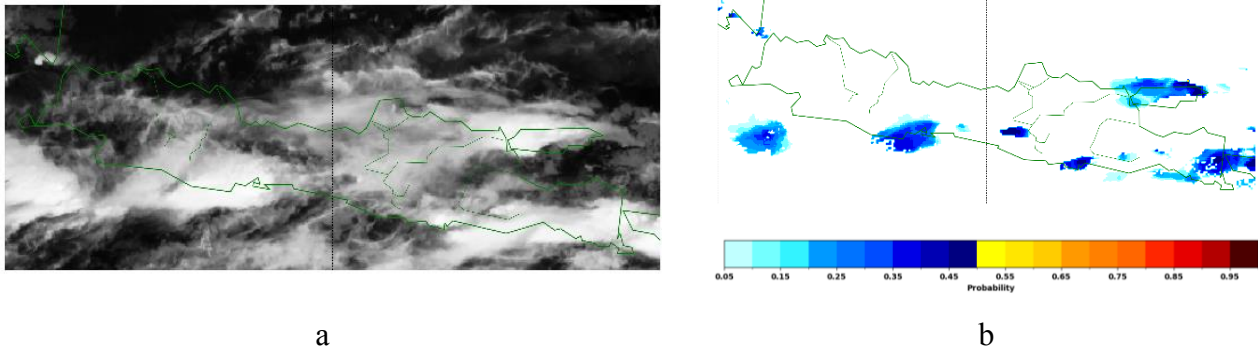
a   b

Figure 1 Example dataset (s) input (b) Ground truth

spatiotemporal sequence problem can be solved using ConvLSTM, as shown in these studies [21].

II. RELATED WORKS

A. Himawari-8

Himawari-8 is the latest generation of Japan's geostationary meteorological satellites operated by the Japan Meteorological Agency (JMA) [23]. Himawari-8 has 16 bands with a spatial resolution of 0.5 to 1 km for the visible and near-infrared bands. In addition, the infrared band s has a spatial resolution of 2 Km.

B. Rapidly Development Cumulus Area (RDCA)

Rapidly Development Cumulus Area was first developed by the Meteorological Satellite Center (MSC) of the Japan Meteorological Agency (JMA). RDCA was developed to predict lightning's appearance using a logistic regression model (LR) [24]. Seven bands owned by Himawari-8, namely bands 03, 08, 10, 11, 13, 15, and 16, produce 13 cloud formation parameters. These parameters are then used to calculate the LR value to create an index RDCA value of 0 to 1. The equation can be seen below,

$$P = \frac{1}{1 + exp\{-(\alpha_0 + \sum_i \alpha_i x_i)\}} \qquad (1)$$

Where α_0 and α_i is the regression coefficient between parameters, x_i is an indicator of lightning detection, and i is the index of each detection indicator. There are 13 detection indicators used in RDCA. More details on the RDCA method can be read in [8]–[10], [24].

C. Convolutional Long-Short Term Memory

Research on convolutional long-short term memory (ConvLSTM) was first introduced by Shi et al.[21]. The authors formulated short-term rainfall forecasting as a spatiotemporal sequence forecasting problem in this study. By expanding fully connected LSTM (FC-LSTM) by adding a convolution process to each cell, the authors introduce a ConvLSTM network. The network structure is divided into two parts, i.e., encoding and forecasting. Each section consists of a stack of ConvLSTM layers along n sequences. With a structure like this, the model has representational solid power, making it suitable for predicting dynamic systems such as rainfall forecasting problems. Same with LSTM,

ConvLSTM has three gates namely input, forget, and output gate. The equations of ConvLSTM are shown below,

$$C_t = f_t \odot c_{t-1} + i_t \odot g_t \qquad (2)$$
$$h_t = o_t \odot tanh(c_t) \qquad (3)$$
$$i_t = \sigma(W_{xi} * x_t + W_{hi} * h_{t-1} + W_{ci} * C_{t-1} + b_i) \qquad (4)$$
$$f_t = \sigma(W_{xf} * x_t + W_{hf} * h_{t-1} + W_{cf} * C_{t-1} + b_f) \qquad (5)$$
$$g_t = tanh(W_{xg} * x_t + W_{hg} * h_{t-1} + b_g) \qquad (6)$$
$$o_t = \sigma(W_{xo} * x_t + W_{ho} * h_{t-1} + W_{co} \odot C_t + b_o) \qquad (7)$$

C_t and h_t are cells and hidden state in time (t). i_t, f_t, and o_t are input gate, forget gate, and output gate in time (t). g_t is the candidate cell in time (t). x_t is input. W_{xi}, W_{xf}, W_{xg}, and W_{xo} are weight input (x) for every component i, f, g, and o. W_{hi}, W_{hf}, W_{hg} and W_{ho} are weight of hidden state (h) for every component i, f, g, and o. W_{ci}, W_{cf}, and W_{co}, is weight output (C) for every component i, f, g, and o. $\odot$ is Harmard. $*$ is a convolution operation.

III. METHOD

A. Dataset

In this study, two data sources were used: data from satellite Himawari-8 and the RDCA model. We download and collect data from January 2021 until February 2021 with time intervals of 10 minutes. As shown in Figure 1 (a), this data is used as input for the prediction model (ConvLSTM) or RDCA model.

The second one is data from the RDCA model, as shown in Figure 1 (b). The result of this model was used as the ground truth of the prediction model (ConvLSTM) so that during the learning process, the model learned to obtain the probability of heavy rainfall like the RDCA model.

There are three stages in the preprocessing dataset. The first stage is resizing the image according to the study area. In this study, the coverage area is 105°E - 115°E, 5°S-9°S, i.e., Java Island, Indonesia. So the data has a grid size of 201x501, represented as i x j, for each data, then described as X for input data and Y for ground truth data where $X, Y \in \mathbb{R}^{i \times j}$. In the second stage, the data are grouped according to their temporal size.

In this study, the minimum temporal size is 16. This aims to keep the data consecutive. The final stage is preparing the sample. In sampling, we use the non-overlapping method. The size of each piece is eight sequences consisting of three input sequences and five output sequences.
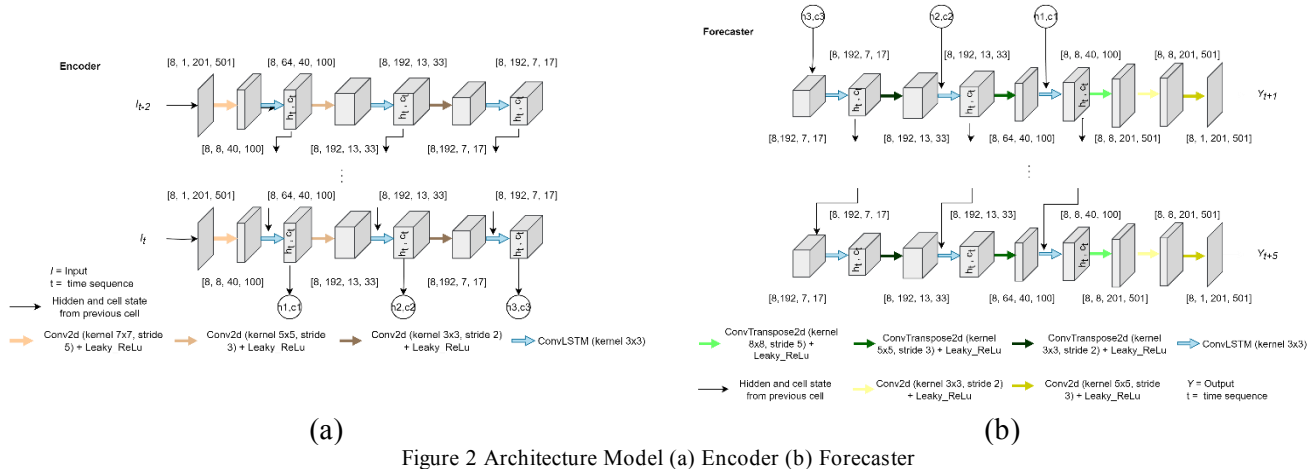
Figure 2 Architecture Model (a) Encoder (b) Forecaster

B. Framework of the Model

In this study, we used ConvLSTM with encoder-forecaster architecture, as shown in Figure 2. The encoder consists of three sequences or 30 minutes of previous brightness temperature from Himawari-8 (band 13). Each sequence has input with shape size [1,201,501] or (batch, height, width). Three layers of ConvLSTM are used, and 2D convolutional operation (down-sampling) with different kernel sizes and strides before the ConvLSTM process.

Whereas the forecaster consists of five sequences or 50 minutes after. The forecaster aims to predict heavy rainfall. Same as input, each output sequence has a shape size [1,201,501]. In the forecaster, there is an up-sampling process after the ConvLSTM process, which aims to restore the image size.

C. Metric Evaluation

In this study, the model is evaluated using computer vision metrics such as the Structural Similarity Index (SSIM) to obtain the level of similarity of ground truth data and prediction results [25]. The equation of SSIM can be seen as follows.

$$SSIM(y,\hat{y}) = \frac{(2\mu_y\mu_{\hat{y}} + C_1)(2\sigma_{y\hat{y}} + C_2)}{(\mu_y^2 + \mu_{\hat{y}}^3 + C_1)(\sigma_y^2 + \sigma_{\hat{y}}^2 + C_2)} \qquad 8$$

where y and $\hat{y}$ are the actual data and prediction data. μ and σ is the average value and variance. C_1 and C_2 is a constant that is $C_1 = (0.01 * L)^2$ and $C_2 = (0.03 * L)^2$ where L is the maximum value of the predicted results.

In addition, statistical metrics are also used to evaluate prediction results. Metrics such as false alarm rate (FAR), probabilities of detection (POD), critical success index (CSI). The equation of the three metrics can be seen as follows.

$$POD = \frac{Hit}{Hit + False\ Alarm} \qquad 9$$

$$FAR = \frac{Miss}{Hit + Miss} \qquad 10$$

$$CSI = \frac{Hit}{Hit + False\ Alarm + Miss} \qquad 11$$

Calculations are performed for each threshold value (0.1, 0.3, 0.5, 0.7, 0.9). For example, for a threshold of 0.1, each grid on observation and prediction data is categorized as positive (1) or negative (0) with positive conditions if p ≥ threshold. Next, in every grid, the observation and prediction data are compared with each other so that a hit value can be obtained, which states the sum of the observed and predicted values which are both positive, miss which is the sum of the observed values which are positive but the predictive value is negative, false alarm which is the sum of the observed value is negative while the prediction is positive, correct non-negative which is the sum of the observed values, and the predicted value are both positive.

D. Simulation

For Training the model, the Dataset has been pre-processed previously divided by the composition of training data, validation data, and test data sequentially 80% (1392), 10% (308), and 10% (308). In addition, each data will use 8 batch groupings so that each iteration will use eight sorted data. In this experiment, we used Adam optimizer with a learning rate 1e-5 by reducing the learning rate every 50 iterations with a gamma value of 0.7.

The training process is carried out by looking at the loss values in the training and validation data. In this study, the calculation of the loss function used is the Balanced Mean Squared Error (BMSE) and Balanced Mean Absolute Error (BMAE) [26]. These two functions are used because the data is imbalanced between categories. This function is similar to the MSE and MAE functions in general. However, the difference lies in the weight given to each value at the threshold. The distribution of weights is determined by the data's probability values, as shown in Table 1.

Table 1 Weight distribution

Probability of Extreme Rain (p)	Data (%)	Weight
$0 \leq p < 0.1$	95,569	1
$0.1 \leq p < 0.3$	2,876	1
$0.3 \leq p < 0.5$	1,495	4
$0.5 \leq p < 0.7$	0.058	8
$0.7 \leq p < 0.9$	0.001	16
$0.9 \leq p \leq 1$	0.001	50

Based on the weights in Table 1, the calculation of the loss function BMSE and BMAE can be formulated as follows

$$BMSE = \frac{1}{N} \sum_{n=1}^{N} \sum_{i=1}^{I} \sum_{j=1}^{J} w_{n,i,j} (y_{n,i,j} - \hat{y}_{n,i,j})^2 \qquad 12$$

$$BMAE = \frac{1}{N} \sum_{n=1}^{N} \sum_{i=1}^{I} \sum_{j=1}^{J} w_{n,i,j} |y_{n,i,j} - \hat{y}_{n,i,j}| \qquad 13$$

Where, $w_{n,i,j}$, $y_{n,i,j}$, and $\hat{y}_{n,i,j}$ respectively are the weight values, actual values, and predicted values of coordinates i,j in the nth sequence. While N, I, and J refer to the sequence size, width, and length of the data.

IV. RESULT AND DISCUSSION

A. Training result

The training process is measured from the loss values generated from the training and validation data. The calculation of the loss function used is the Balanced Mean Squared Error (B-MSE) and Balanced Mean Absolute Error (B-MAE), whose equations can be seen in 12 and 13. The loss value obtained at this stage is seen in Figure 3. Based on the loss graph obtained, there is a decrease in the loss value, which indicates that the model is approaching its convergence, and in the training process, the model is doing well.
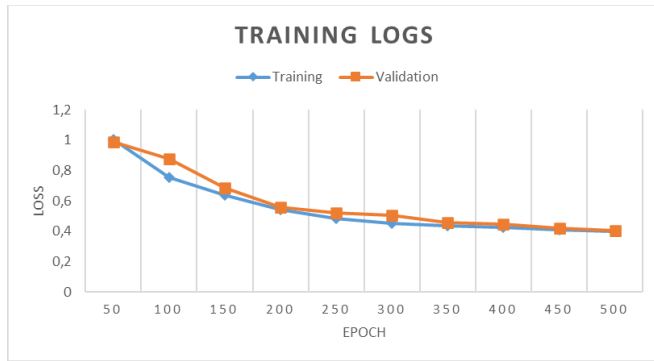

Figure 3 ConvLSTM training and validation losses over time

B. Spatial comparison between the RDCA indices and the ConvLSTM Model
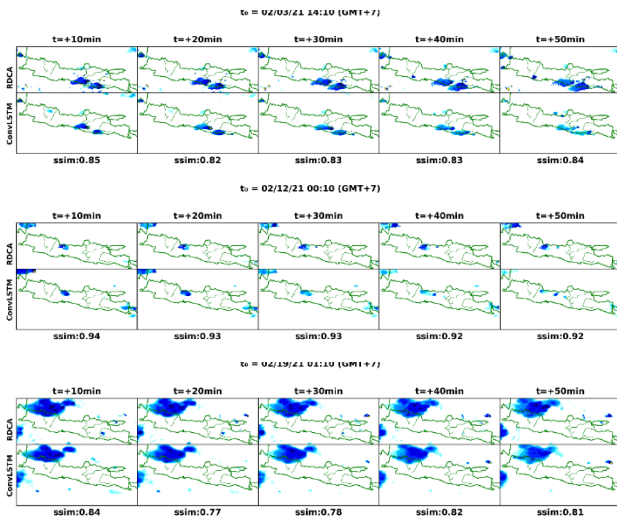

Figure 4 Comparison between the predicted results of the RDCA and the ConvLSTM model

In addition to producing a predictive model that can predict extreme rainfall, this research is also expected to solve problems in the RDCA prediction model, which has not been able to make predictions for some time. To see how good the model is, we compare the output of the model we built with the RDCA model. The comparison can be seen in Figure 4. We present three comparison examples on 03-02-2021 14:10 WIB, 12-02-2021 00:10 WIB, and 19-02-2021 01:10 WIB with time frames up to t+50. From this figure, the model can be said to be good at predicting rainfall. This can also be seen from the average value of SSIM is above 0.8. It means that the predicted image is similar to the ground truth.

C. Study Case

One of the case studies we observed to evaluate this model's performance is the flood disaster in Cibunian village, Bogor City, West Java, Indonesia. This incident occurred on June 22, 2022. Based on observations of estimated rainfall from GSMaP (Global Satellite Measurement of Precipitation) in Figure 5, rainfall occurs from 16:00 WIB to 17:00 WIB.
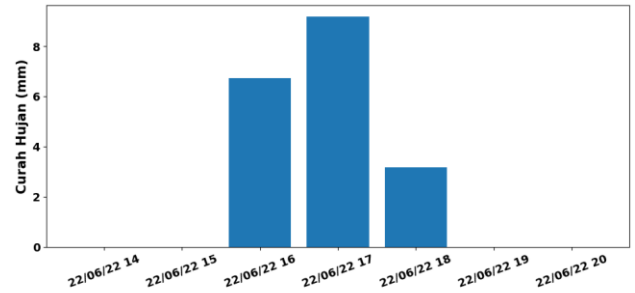

Figure 5 Rainfall Observations from GSMaP data for the Bogor City case study

As can be seen from the results of the prediction model built as shown in Figure 6, the model recognizes the possibility of convection forming, which can cause rain at t = 16:10, which then convection enlarges and expands over time. Using this prediction model, we can see an increase in probability over time. This probability is closely related to the rainfall that will occur.

D. Evaluation

Overall evaluation can be seen in Table 2 and Table 3. Threshold ≥ 0.1 indicates rain activity in the study area. The greater the threshold value, the fewer rainfall probability categories are observed. From 10 to 50 minutes, the highest POD and CSI values were obtained at the threshold = 0.1 with an average of 0.6 and 0.5. These results indicate that the prediction model performs reasonably well in detecting the occurrence of rainfall. These values decrease with increasing value threshold to be observed, and the lowest value is obtained at
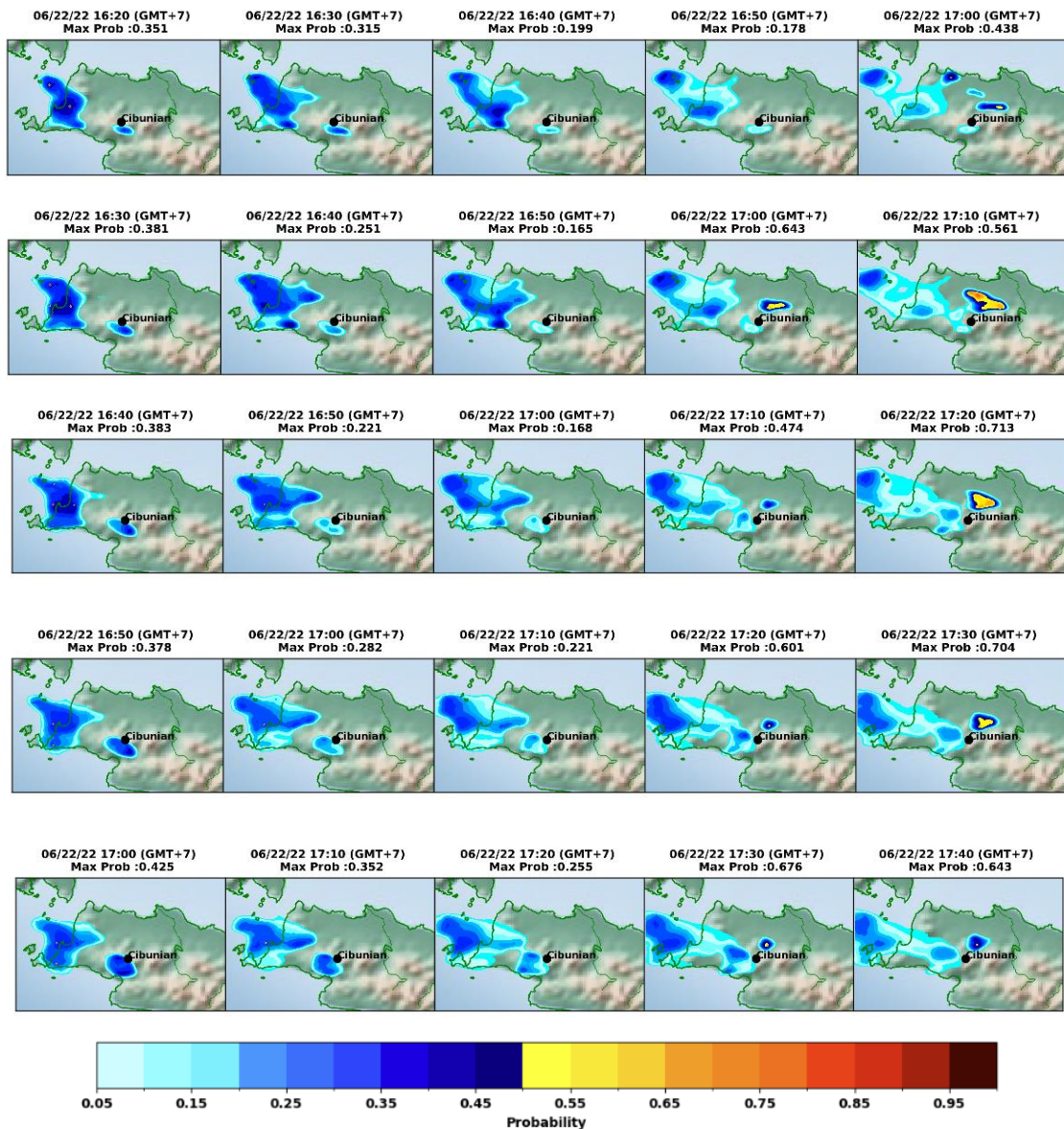
Figure 6 Predictive results for the Bogor City flood case study

threshold = 0.7, where the average POD and CSI values obtained are only around 0.06 and 0.03. These results indicate that the model performs very poorly in detecting high rainfall. Apart from that, the average accuracy of the model obtained is around 90% for each threshold value. High accuracy but lower in sensitivity (POD) indicates the model is good for predict rainfall in general but not effectively identifying a positive instance. Therefore, there is still room to improve the model's prediction performance to enhance the results.

Table 2 POD, FAR, and CSI value for each lead time (thresholds 0.1 and 0.3)

Time (min)	Threshold = 0.1			Threshold = 0.3		
	POD	FAR	CSI	POD	FAR	CSI
t= + 10min	0.689	0.353	0.501	0.462	0.497	0.317
t=+ 20min	0.686	0.348	0.502	0.426	0.435	0.320
t= + 30min	0.647	0.352	0.479	0.372	0.423	0.292
t=+ 40min	0.592	0.386	0.432	0.339	0.490	0.256
t=+ 50min	0.478	0.429	0.352	0.267	0.567	0.198

Table 3 POD, FAR, and CSI value for each lead time (thresholds 0.5 and 0.7)

Time (min)	Threshold = 0.5	Threshold = 0.7

	POD	FAR	CSI	POD	FAR	CSI
t= + 10min	0.076	0.886	0.048	0.018	0.984	0.009
t=+ 20min	0.160	0.778	0.103	0.064	0.895	0.041
t= + 30min	0.197	0.744	0.125	0.086	0.875	0.054
t=+ 40min	0.182	0.789	0.108	0.080	0.914	0.043
t=+ 50min	0.136	0.843	0.079	0.070	0.936	0.035

V. CONCLUSIONS AND FUTURE WORK

In this study, we demonstrate that ConvLSTM are capable of predict rainfall using Himawari-8 and RDCA data. This can be seen from the good CSI, POD, and FAR evaluation values for several threshold values. Although, for thresholds, the results are still not good. As an early warning system, this prediction model can be used as one of the decision considerations. By observing rainfall conditions in disaster-prone areas, decision-makers can keep rainfall conditions for some time to provide time for making decisions in disaster mitigation.

Suggestions that can be given in this research is additional pre-processing method is needed to handle imbalance data, especially for data with an RDCA index value greater than 0.5.

REFERENCES

[1] BNPB, "DATA BENCANA INDONESIA 2022," Jakarta. Accessed: Jul. 10, 2023. [Online]. Available: https://perpustakaan.bnpb.go.id/

[2] Meilani Safira Indradewa, "Potensi dan upaya penanggulangan bencana banjir sungai wolowona, nangaba dan kaliputih di Kabupaten Ende," 2013, UNIVERSITAS SEBELAS MARET, UNIVERSITAS SEBELAS MARET, 2013.

[3] M. Hattori, S. Mori, and J. Matsumoto, "The cross-equatorial northerly surge over the maritime continent and its relationship to precipitation patterns," *Journal of the Meteorological Society of Japan*, vol. 89, no. A, pp. 27–47, 2011, doi: 10.2151/JMSJ.2011-A02.

[4] S. Mori *et al.*, "Lightning climatology over Jakarta, Indonesia, based on long-term surface operational, satellite, and campaign observations," 2016.

[5] S. Mori *et al.*, "Meridional march of diurnal rainfall over Jakarta, Indonesia, observed with a C-band Doppler radar: an overview of the HARIMAU2010 campaign," *Prog Earth Planet Sci*, vol. 5, no. 1, Dec. 2018, doi: 10.1186/S40645-018-0202-9.

[6] W. Fang, Q. Xue, L. Shen, and V. S. Sheng, "Survey on the Application of Deep Learning in Extreme Weather Prediction," *Atmosphere (Basel)*, vol. 12, no. 6, p. 661, May 2021, doi: 10.3390/atmos12060661.

[7] P. Lynch, "The origins of computer weather prediction and climate modeling," *J Comput Phys*, vol. 227, no. 7, pp. 3431–3444, Mar. 2008, doi: 10.1016/j.jcp.2007.02.034.

[8] W. Harjupa, E. Nakakita, Y. Sumida, and K. Yamaguchi, "Fundamental Investigation Of Generation Of Guerilla-Heavy Rainfall Using Himawari-8 And Xrain Information In Kinki Region," *Journal of Japan Society of Civil Engineers, Ser. B1 (Hydraulic Engineering)*, vol. 74, no. 4, p. I_283-I_288, 2018, doi: 10.2208/jscejhe.74.I_283.

[9] W. Harjupa, E. Nakakita, Y. Sumida, and A. Masuda, "Trial Utilization Of Rapid Scan Observation Of Himawari-8 For Obtaining Information On Cumulus Life Stage," *Journal of Japan Society of Civil Engineers, Ser. B1 (Hydraulic Engineering)*, vol. 74, no. 5, p. I_283-I_288, 2018, doi: 10.2208/jscejhe.74.5_I_283.

[10] W. Harjupa, E. Bakakita, Y. Sumida, and A. Masuda, "RDCA Index Based Updraft Area And Its Verification Using Polarimetric Doppler Radar," *Journal of Japan Society of Civil Engineers, Ser. B1 (Hydraulic Engineering)*, vol. 75, no. 2, p. I_127-I_132, 2019, doi: 10.2208/jscejhe.75.2_I_127.

[11] Y. LeCun, Y. Bengio, and G. Hinton, "Deep learning," *Nature*, vol. 521, no. 7553, pp. 436–444, May 2015, doi: 10.1038/nature14539.

[12] A. Krizhevsky, I. Sutskever, and G. E. Hinton, "ImageNet classification with deep convolutional neural networks," *Commun ACM*, vol. 60, no. 6, pp. 84–90, Jun. 2017, doi: 10.1145/3065386.

[13] D. Amodei *et al.*, "Deep Speech 2: End-to-End Speech Recognition in English and Mandarin," *33rd International Conference on Machine Learning, ICML 2016*, vol. 1, pp. 312–321, Dec. 2015, Accessed: Feb. 23, 2022. [Online]. Available: https://arxiv.org/abs/1512.02595v1

[14] A. X. Lee, R. Zhang, F. Ebert, P. Abbeel, C. Finn, and S. Levine, "Stochastic Adversarial Video Prediction," Apr. 2018, Accessed: Feb. 23, 2022. [Online]. Available: https://arxiv.org/abs/1804.01523v1

[15] M. Mathieu, C. Couprie, and Y. LeCun, "Deep multi-scale video prediction beyond mean square error," *4th International Conference on Learning Representations, ICLR 2016 - Conference Track Proceedings*, Nov. 2015, Accessed: Feb. 23, 2022. [Online]. Available: https://arxiv.org/abs/1511.05440v6

[16] L. Alzubaidi *et al.*, "Review of deep learning: concepts, CNN architectures, challenges, applications, future directions," *Journal of Big Data 2021 8:1*, vol. 8, no. 1, pp. 1–74, Mar. 2021, doi: 10.1186/S40537-021-00444-8.

[17] M. I. Khan and R. Maity, "Hybrid Deep Learning Approach for Multi-Step-Ahead Daily Rainfall Prediction Using GCM Simulations," *IEEE Access*, vol. 8, pp. 52774–52784, 2020, doi: 10.1109/ACCESS.2020.2980977.

[18] A. Khan, A. Sohail, U. Zahoora, and A. S. Qureshi, "A survey of the recent architectures of deep convolutional neural networks," *Artificial Intelligence Review 2020 53:8*, vol. 53, no. 8, pp. 5455–5516, Apr. 2020, doi: 10.1007/S10462-020-09825-6.

[19] K. Lee, C. Choi, D. H. Shin, and H. S. Kim, "Prediction of Heavy Rain Damage Using Deep Learning," *Water (Basel)*, vol. 12, no. 7, p. 1942, Jul. 2020, doi: 10.3390/w12071942.

[20] S. Agrawal, L. Barrington, C. Bromberg, J. Burge, C. Gazen, and J. Hickey, "Machine Learning for Precipitation Nowcasting from Radar Images."

[21] X. Shi, Z. Chen, H. Wang, D. Y. Yeung, W. K. Wong, and W. C. Woo, "Convolutional LSTM Network: A Machine Learning Approach for Precipitation Nowcasting," *Adv Neural Inf Process Syst*, vol. 2015-January, pp. 802–810, Jun. 2015, Accessed: Jul. 26, 2023. [Online]. Available: https://arxiv.org/abs/1506.04214v2

[22] S. Hochreiter and J. Schmidhuber, "Long Short-Term Memory," *Neural Comput*, vol. 9, no. 8, pp. 1735–1780, Nov. 1997, doi: 10.1162/neco.1997.9.8.1735.

[23] K. BESSHO *et al.*, "An Introduction to Himawari-8/9&mdash; Japan&rsquo;s New-Generation Geostationary Meteorological Satellites," *Journal of the Meteorological Society of Japan. Ser. II*, vol. 94, no. 2, pp. 151–183, 2016, doi: 10.2151/jmsj.2016-009.

[24] Y. Sumida, H. Suzue, T. Imai, and A. Sobajima, "Convective cloud information derived from Himawari-8 data," 気象衛星センター技術報告= *Meteorological Satellite Center technical note/ 気象衛星センター 編*, no. 62, pp. 19–37, 2017.

[25] Z. Wang, A. C. Bovik, H. R. Sheikh, and E. P. Simoncelli, "Image quality assessment: From error visibility to structural similarity," *IEEE Transactions on Image Processing*, vol. 13, no. 4, pp. 600–612, Apr. 2004, doi: 10.1109/TIP.2003.819861.

[26] X. Shi *et al.*, "Deep Learning for Precipitation Nowcasting: A Benchmark and A New Model," *Adv Neural Inf Process Syst*, vol. 2017-December, pp. 5618–5628, Jun. 2017, Accessed: Jul. 26, 2023. [Online]. Available: https://arxiv.org/abs/1706.03458v2